NASA Technical Memorandum 82806

Strength Advantages of Chemically Polished Boron Fibers Before and After Reaction with Aluminum

James A. DiCarlo and Robert J. Smith
Lewis Research Center
Cleveland, Ohio

Prepared for the
Sixth Annual Conference on Composites and Advanced Materials
sponsored by the American Ceramic Society
Cocoa Beach, Florida, January 18-21, 1982

NASA

STRENGTH ADVANTAGES OF CHEMICALLY POLISHED BORON FIBERS BEFORE AND AFTER REACTION WITH ALUMINUM

by James A. DiCarlo and Robert J. Smith

National Aeronautics and Space Administration
Lewis Research Center
Cleveland, Ohio 44135

ABSTRACT

In order to determine their strength potential, the fracture properties of different types of commercial boron fibers were measured before and after application of secondary strengthening treatments. The principal treatments employed were a slight chemical polish, which removed low strength surface flaws, and a heat treatment in oxygen, which contracted the fibers and thereby compressed intrinsic bulk flaws. Those fiber types most significantly strengthened were 200 to 400 μm (8 to 16 mil) diameter boron on tungsten fibers produced in a single chemical vapor deposition reactor. The slight polish increased average tensile strengths from 3.4 to 4.4 GN/m^2 (500 to 640 ksi) and reduced coefficients of variation from about 15 to 3 percent. The oxygen heat treatment plus slight polish further improved average strengths to 5.5 GN/m^2 (800 ksi) with coefficients near 3 percent. To ascertain whether these excellent properties could be retained after fabrication of B/Al composites, as-produced and polished 203 μm (8 mil) fibers were thinly coated with aluminum, heat treated at B/Al fabrication temperatures, and then tested in tension and flexure at room temperature. The pre-polished fibers were observed to retain their superior strengths to higher temperatures than the as-produced fibers even though both were subjected to the same detrimental reaction with aluminum. The practical implications of the strength results are discussed with particular emphasis on the potential of fabricating high strength high-impact resistant B/Al composites.

E-1146

INTRODUCTION

Because of their high stiffness and strength-to-weight ratios, boron/aluminum (B/Al) composites are replacing monolithic metallic materials in many structural applications. However, for impact-prone structures, such as the fan blades of gas turbine engines, this replacement process has been delayed somewhat by the fact that B/Al composites of recent production have displayed low mechanical energy absorption capability during impact. Simple composite deformation theory indicates that some improvement in energy absorption could be achieved by increasing such parameters as fiber diameter and matrix ductility, but that major improvements would result if the boron fiber strength within B/Al composites could be significantly increased above current levels (1,2). In general this could be accomplished by the development of fiber and composite processing treatments which improve the tensile strength of currently available boron fibers and which allow retention of this higher strength under the high temperature conditions encountered during fabrication of B/Al composites.

Over the last two decades improvements in production techniques have resulted in commercial boron fibers with average tensile strengths consistently near 3.4 GN/m^2 (500 ksi) (3). However, this strength level is well below the theoretical strength for boron estimated at 40 GN/m^2 (5800 ksi) or 10 percent of the fiber modulus, indicating that currently available fibers are still limited by production related flaws. In an effort to identify and possibly eliminate some of these flaws, Smith (4) studied the fracture characteristics of various small diameter boron on tungsten fibers after subjecting them to a chemical polishing treatment in nitric acid. For a very slight polish he observed the average tensile strength of certain 203 μm (8 mil) fibers to increase from ~3.4 GN/m^2 (500 ksi) to 4.4 GN/m^2 (640 ksi), and the strength coefficient of variation (CV) to decrease from about 15 percent to less than 5 percent. Fracture surface studied indicated that this strength improvement was accompanied by a change in the fatal flaw site from the fiber surface to within the tungsten-boride core. Similar dramatic improvements were not observed for smaller diameter commercial fibers, suggesting that these contained additional strength-limiting flaws weaker than the core flaw.

By polishing deeper into the sheath of the 203 μm (8 mil) fibers, Smith found the tensile strength to increase further, reaching 5.5 GN/m^2 (800 ksi) at a reduced diameter of 100 μm (4 mil). Throughout the deep polish the CV remained below 5 percent and the fatal flaws were always within the fiber core. The strengthening mechanism during deep polishing was proven by Behrendt (5) to be due to core compression caused by an axial contraction of the fiber as outer layers of the boron sheath were removed. Core compression by axial contraction was later utilized by DiCarlo (6) to develop secondary strengthening treatments other than the deep polish. The most cost effective was an oxidation plus polishing treatment (7) which provided 5.5 GN/m^2 (800 ksi) fibers with CV near 3 percent. Thus, for at least some types of commercial boron fibers, secondary processing treatments do exist which can substantially minimize the effects of production related strength-limiting flaws.

Whether the strength improvement gained by these secondary treatments could be retained after fabrication of B/Al composites was not determined. It is well known that during high temperature B/Al fabrication and use, losses in fiber strength can occur due to the thermally-induced formation of weak boron-aluminum reaction phases on the fiber surface (8). For small reaction zone thicknesses, the fiber exhibits its original strength because reaction-induced flaws are still stronger than the intrinsic fiber flaws. Above some threshold thickness, however, the fiber strength becomes limited by reaction flaws and decreases monotonically as the reaction zone thickness increases (8). The fact that fibers removed from B/Al composites typically display strengths lower than their original strengths (9) indicates that composite fabricators have been forced to accept reaction zone thicknesses larger than the threshold thicknesses for as-produced strengths near 3.4 GN/m^2 (500 ksi). Presumably this is a consequence of the high temperatures required for complete diffusion bonding of the aluminum matrix. If such large reaction zones are a necessary part of B/Al fabrication conditions, it is unclear whether original fiber strengths well over 3.4 GN/m^2 (500 ksi) could indeed be maintained.

The objectives of the present study were twofold. The first objective was to identify those types of commercially available boron fibers whose

strength properties were most likely to be significantly enhanced by the strengthening methods of chemical polishing and axial contraction. Of particular concern were those fibers with diameters larger than 203 μm (8 mil) since there is experimental evidence that the impact energy absorption capability of B/Al composites improves not only with fiber strength but also with fiber diameter (1,10). The second objective was to determine whether the excellent strength properties associated with core-initiated fracture could indeed be maintained under typical thermal processing conditions encountered in the fabrication of B/Al composites. Because of the complications involved in interpreting the sources of tensile failure for multifiber-reinforced composites, the approach taken was to ion plate individual 203 μm (8 mil) diameter fibers with aluminum at low temperature and then to measure the strength characteristics of the coated fiber after heat treatment at B/Al fabrication temperatures. By coating both as-produced fibers and strengthened polished fibers and then heating both types under the same time-temperature conditions, direct comparisons could be made of the effects of thermal degradation on fiber strength.

EXPERIMENTAL PROCEDURE

Specimen Preparation

Table I lists the types of commercial boron fibers surveyed for the purpose of determining strengthening potential by secondary processing. As indicated, the fiber types differed primarily in four ways: diameter, substrate or core material, manufacturing source, and production method. Also included is the notation used to distinguish each fiber type; that is, the first number is the diameter in mils and the second letter the chemical symbol for the substrate. The two manufacturing sources, Avco Speciality Materials (AVCO) and Composite Technology Incorporated (CTI), are distinguished, respectively, by the absence or presence of an asterisk.

Regarding production methods, all fibers were produced continuously in a chemical vapor deposition (CVD) reactor by the hydrogen reduction of boron trichloride onto a small diameter wire. Deposition temperatures were maintained near 1300° C (2370° F) by dc resistance heating of the substrate and deposited boron. In most cases the substrate was 13 μm (0.5 mil) diameter tungsten (W) wire which became completely borided to form a 17 μm (0.7 mil) tungsten-boride core at the fiber axis. To reduce total fiber cost, AVCO has also deposited boron on a 33 μm (1.3 mil) carbon (C) monofilament substrate which is mechanically decoupled from the boron sheath by a 2.5 μm (0.1 mil) thick coating of pyrolytic graphite (3). For production efficiency, the 102 and 142 μm (4 and 5.6 mil) diameter fibers were deposited in a single CVD reactor with a single internal heating stage (SRSS); whereas the larger diameter fibers were deposited in a single reactor with multiple stages (SRMS) or in a double reactor with single stages (DRSS). For this latter process which was employed for the 8W fibers, a small diameter fiber previously produced in a single stage reactor was passed through a second reactor to increase diameter. An exception was the ACVO 8W fiber which was deposited in a single-stage single-reactor by augmenting the dc heating by high frequency heating (3).

The chemical polish treatment was that used by Smith (4) in which short lengths of fiber are immersed in a solution of two parts by volume nitric

acid and one part water. For a solution temperature of 98° C (208° F), approximately 25 μm (1 mil) was removed from the fiber diameter for every 5 minutes of immersion time. Polished specimens were rinsed in water and wiped with methanol before tensile testing.

For the study of aluminum interaction effects, 10 cm (4 in.) long as-produced and polished type 8W fibers were cleaned in methanol and inserted into the ion-plating specimen holder shown in Fig. 1. The holder consisted of a cylindrical metal screen with brass end caps that supported and separated the fibers. The ion-plating technique was that employed by Spalvins (11). The screen was attached to an electrode in the center of a vacuum chamber which was first evacuated and then back filled with argon at about 3 N/m^2 (0.025 torr) pressure. At electrode potentials near 800 volts, a glow discharge was produced in the argon. Aluminum atoms evaporated from a heated boat below the holder were ionized by the argon ions, electrically attracted to the screen, and ion plated uniformly onto the fiber surfaces. The maximum fiber temperature produced by the impinging aluminum atoms was estimated to be less than 300° C (570° F). Final coating thickness ranged between 2 and 4 μm (0.08 and 0.16 mil).

Heat treatment at B/Al fabrication temperatures was accomplished by placing the coated fibers, both as-produced and pre-polished, in a quartz tube, evacuating the tube to about 10^{-6} N/m^2 (10^{-8} torr) dynamic pressure, and heating the tube in a furnace for 1 hour at various temperatures. Temperature was maintained to within ±2° C (4° F) as monitored by a ceramic-sheathed thermocouple situated next to the fibers.

Strength Measurement

The stress levels required to fracture uncoated and aluminum-coated boron fibers were measured both in tension and bending at room temperature. For the tensile strength measurements, specimen gauge lengths were 25 and 250 mm (1 and 10 in.) for uncoated fibers, but only 25 mm (1 in.) for coated fibers. Fiber gripping was achieved in flat steel pneumatic grips lined with 127 μm (5 mil) aluminum sheet. In most cases the gauge section of the fiber was coated with vacuum grease to retain the original fracture surfaces. Optical microscopy was subsequently used to examine the fracture surfaces and identify the site of the strength-limiting flaw. Strain rate for the tensile tests was 0.2 percent/min. Errors in the fracture stress calculations caused by measurement errors in load and diameter were estimated to be less than 2 percent.

Flexure strength measurements were performed by bending fibers around a cone-shaped brass mandrel. From base to apex, the cone diameter $2a$ decreased in discrete steps of $\Delta(2a) = 0.76$ mm (0.030 mils). Starting at the lowest step, each fiber was bent by light finger pressure around a semicircle of length πa. If fracture did not occur, the fiber was raised without rotating to the next smaller diameter step and the bending process repeated until fracture occurred. The flexural strength σ_b was calculated from the maximum bending strain on the fiber surface:

$$\sigma_b = \frac{ED}{2a} \qquad (1)$$

where E is the fiber modulus taken as 400 GN/m^2 (58 Msi), D is the fiber diameter, and $2a$ was taken as the smallest cone diameter at which the fiber did not fracture. Thus the calculated σ_b slightly underestimated the true flexural strength. The error introduced by this effect amounted to ~3 percent for as-produced and heat-treated fibers and ~6 percent for polished fibers.

For fibers prepared in exactly the same manner, a scatter in individual tensile strengths was observed, presumably caused by a distribution in both size and location of strength-limiting flaws. Because this effect implies that the average fiber strength will vary with gauge length, it was necessary to employ statistical fracture theory in order to predict the tensile results to be expected at gauge lengths other than those actually employed. The approach taken in this study was to assume the strength data could be fitted to two-parameter Weibull theory (12) which predicts that average tensile strength $\bar{\sigma}_L$ at gauge length L obeys the relation

$$\bar{\sigma}_L = \gamma(L)^{-1/\omega}. \tag{2}$$

Here γ is a scale parameter, and ω is the Weibull modulus which can be obtained from the coefficient of variation (CV):

$$CV \equiv \frac{(SD)_L}{\bar{\sigma}_L} = \frac{1.2}{\omega} \tag{3}$$

where $(SD)_L$ is the standard deviation in tensile strength data measured at constant L.

Unlike the tensile tests, the gauge lengths in the bending tests were not constant within a test group and the applied stresses were not constant across the fiber cross section. If strength-limiting flaws were distributed along the fiber length and also across fiber cross section, statistical analysis of the flexure strength data would be very difficult. However, in this study fiber fracture was often controlled only by surface flaws. For this situation the Appendix A shows that two-parameter Weibull theory can be used to correct for the bend test problems, thereby allowing the flexure data to be treated as the tensile data to be expected at an effective gauge length L^*. Typically the L^* values for this study were near 2.5 mm (0.1 in.) so that, as predicted by Eq. (2), the average flexure strengths were observed to be larger than the average tensile strengths measured at L = 25 mm (1 in.).

RESULTS AND DISCUSSION

Strengthening of Commercial Fibers

Type 8W fibers. - The improvement in strength properties to be achieved by a chemical polish treatment was first demonstrated by Smith (4) using type 8W fibers. Tensile strength results for this fiber type are summarized in Table II in terms of average strength $\bar{\sigma}$ at gauge lengths L of 25 and 250 mm (1 and 10 in.) and at various polished diameter ratios D/D_o

where D_o is the original as-produced diameter. Also included in the table are the coefficients of variation (CV); the maximum and minimum strengths, σ_{max} and σ_{min}; and the number of specimens within a test group.

Fracture surface examination of the 8W fibers indicated that the flaws responsible for the low and high strength values of the as-produced fibers were located on the fiber surface and within the tungsten-boride core, respectively. After slight or deep polishing, the fatal flaws were found only within the core. Thus the Table II results which indicate strengthening after removal of only a few μm of surface material can be explained simply by the elimination of low-strength surface flaws. The further strengthening observed after deep polishing was proven by Behrendt (5) to be due to a mechanical compression of the core created by an axial contraction of the boron sheath during polishing. The contraction was caused by removal of surface sheath layers which were placed under residual compression during fiber production. The Table II data for average tensile strength at 25 mm (1 in.) gauge length are plotted as the open circles in Fig. 2. By utilizing Behrendt's results for axial contraction ϵ_z as a function of D/D_o for the 8W fibers, it can be shown that the gradual increase in fiber strength $\Delta\sigma$ obeys the relation $\Delta\sigma = E\epsilon_z$.

To understand the manner in which polishing affects surface flaws, flexure strength properties of the 8W fibers were measured as a function of polished diameter ratio. For the bend tests the applied stresses on the core were near zero so that all bend fractures were presumably initiated by flaws on or near the fiber surface. The flexure results, listed in Table III, show that the average strength $\bar{\sigma}_b$ increased rapidly from about 6 to 12 GN/m^2 (900 to 1700 ksi) during slight polishing and then remained essentially constant during subsequent deep polishing. This behavior is very similar to that observed by Wawner (13) who chemically polished early-production 250 to 380 μm (10 to 15 mil) diameter boron fibers with nitric acid and found $\bar{\sigma}_b$ to level off near 13 GN/m^2 (1900 ksi). As suggested by Wawner, surface-initiated fracture for the as-produced fibers was most probably associated with the crack-like structure of the "kernels" or growth nodules typically found on the surfaces of CVD boron fibers. Examples of these nodules for the 8W fibers in the as-produced and slightly-polished conditions are shown in the optical micrographs of Figs. 3(a) and (b), respectively. The fact that these micrographs, taken with oblique angle lighting, show little change in nodule height after flexure strength doubled suggests that chemical polishing has its major strengthening effect at the nodule boundaries, possibly blunting the crack tips formed at the boundaries.

Comparing the Tables II and III data, one observes that for the as-produced condition the average stress for surface-initiated fracture for the 25 mm (1 in.) gauge length tensile test was about a factor of 0.6 smaller than that measured in the bend test. This difference can be explained by a smaller effective test length of the bend specimens coupled with distributions in flaw strength and location on the fiber surface (cf. Appendix A). The flexure data of Table III multiplied by 0.6 is thus a crude approximation of what might be expected in a 25 mm (1 in.) gauge length tensile test if fracture were only controlled by surface flaws. It follows then from the flexure data that slight polishing produced a significant increase in the average stress level for surface-initiated fracture from ~3.5 GN/m^2 (500 ksi) to ~7 GN/m^2 (1000 ksi) but that this high level was not observed

in the tensile data because of the intrinsic core flaw which limited strengths to near 5 GN/m^2 (700 ksi). It also follows that even if the core flaws could be eliminated, boron fibers chemically polished with nitric acid would have an upper surface-controlled limit for average tensile strength of ~7 GN/m^2 (1000 ksi) for a 25 mm (1 in.) test length.

Other fiber types. - The average strength and CV results for all fiber types tested in this study are summarized in Table IV for both the as-produced and slightly-polished conditions. Also included in the table are the results of fracture surface studies to identify fatal flaw sites in the slightly-polished fibers. In general these flaws were located within the core (c), near the core-sheath interface (ci), and at the double-reactor interface (ri) within the sheath.

In the as-produced condition the boron-on-tungsten (B/W) fibers generally display lower average tensile strengths than the boron-on-carbon (B/C) fibers. Fracture surface observations indicated that this effect was caused by a higher incidence of low strength surface-initiated fracture. An understanding of the probable physical source of this substrate-related effect can be obtained from the optical micrographs of Fig. 4 which show the as-produced surface morphology for various fiber types. As explained by Krukonis (3) and in more detail by Vega-Boggio, et al. (14), the nodule surface structure reflects to some degree the morphology of the substrate surface. This is especially evident for the 4W and 5.6W fibers where nodule rows along the fiber axes reflect boron growth from within the die mark groves on the original tungsten wire surfaces. Because boron growth extends radially from a die mark groove, the 5.6W fibers typically have wider and higher nodules than the 4W fibers. For diameters larger than the 5.6W fibers, Figs. 3 and 4 show that nodule dimensions are more random and sub-nodular growth is apparent. An exception is the crystalline-like surface of the 16W* fibers which probably accounts for its very low as-produced strength. The B/C fibers, on the other hand, display a much finer nodule structure, reflecting the relative smoothness of the pyrolytic graphite layer on the carbon substrate wire. Comparing the Table IV results with the surface structures of Figs. 3 and 4, one finds that as-produced strength can be correlated with nodule size; that is, the smaller the average nodule size the greater the as-produced strength. This correlation thus supports Wawner's model that the stresses required for as-produced fiber fracture are primarily controlled by nodule structure (13).

Regarding the effects of polishing on the B/W fibers, the Table IV data show that although polishing strengthened the 4W and 5.6W single-reactor fibers and the 8WD double-reactor fibers, their $\bar{\sigma}$ and CV did not attain the excellent values obtained in the 8W, 8W*, 11W*, and 16W* fiber types. This effect was caused by the measurement of a few low strength values which were not the result of core-initiated fracture. Fracture surface studies on these low strength fibers revealed that the fatal flaw sites were near the core-sheath interface for the small diameter fibers and at the interface between the two sheath layers for the double-reactor fibers. These observations suggest that the smaller diameter B/W fibers possibly contained "proximate voids" (13,14) which were not completely eliminated by diffusion processes. On the other hand, the double-reactor large diameter fibers appeared to be subject to some internal sheath flaw which was created on the surface of the first reactor fiber before or during its passage through the second reactor.

The fact that fracture of the polished large diameter single reactor (LDSR) fibers was core controlled suggested that these fibers could be further strengthened by axial contraction processing treatments (6). To verify this, the tensile strength properties of LDSR fibers were measured after deep polishing treatments and after thermal treatment in oxygen. The deep polishing results are listed in Table V and compared in Fig. 2 with data on the type 8W fibers. Figure 2 shows that during deep polishing all LDSR fibers displayed similar strengthening curves, differing only by slight vertical shifts. On the practical side, these results indeed show the utility of contraction treatments to increase fiber strength. On the basic side, the close agreement in curve shapes suggests very similar residual stress patterns in the outer sheath layers of the different fiber types. The vertical shifts suggest different residual compression states of the tungsten-boride core in the as-produced fibers.

The utility of contraction processing methods for the LDSR boron on tungsten fibers was also confirmed by the Table VI tensile results obtained after application of the oxygen plus slight polish treatments (7). Table VI lists both the oxidation-induced axial contraction strain ϵ_z and the diameter ratio D/D_o measured after polishing. As with deep polishing, the core-controlled strengths increased by the product $E\epsilon_z$ and the CV remained near 3 percent. But unlike deep polishing, only a small fraction of the fiber cross section was removed. The data of Table VI represent the optimum strength properties that have currently been obtained by the oxidation treatment. Although larger contractions could easily be achieved, above $\epsilon_z = 0.3$ percent new flaws weaker than the core flaw began to form at the core-sheath interface (7). Nevertheless, boron fibers with an average strength near 5.5 GN/m^2 (800 ksi) and a diameter of 406 μm (16 mils) may be the strongest large diameter fibers in existence today.

To put the B/W strength results into prospective and also indicate expected gauge length dependences, log $\bar{\sigma}$ data for the LDSR fibers are plotted as a function of log L in Fig. 5. Data for as-produced and slightly-polished fibers are shown by closed and open points, respectively. Because in most cases data were obtained at only one gauge length, a short line segment is drawn through each point to indicate the linear gauge length dependence to be expected using the CV results and Weibull theory (cf. Eqs. (2) and (3)). For as-produced fibers, Table IV and Fig. 5 show that the higher the strength at $L = 25$ mm (1 in.), the lower the CV and the smaller the dependence of σ on L. This effect is a result of the fact that both surface and core flaws contributed to the fracture of most as-produced fibers. Those fibers with rough surfaces displayed surface-initiated fracture characterized by CV from 10 to 20 percent and corresponding Weibull moduli ω from 12 to 6. A typical example of the gauge length dependence for these fiber types is shown by the straight line through the Street and Ferte data for as-produced type 5.6W* fibers (9). On the other hand, those fibers with relatively smooth surfaces tended to display as-produced strength properties closer to those associated with core-initiated fracture; that is, CV near 3 percent and ω near 40. The hatched area in Fig. 5 represents the optimum strength levels to be expected for as-produced B/W fibers with either smooth or slightly-polished surfaces. Finally, because their fracture was core-initiated, the oxygen-treated fibers displayed CV, ω, and gauge length dependence similar to those of the slightly-polished fibers. However, because their cores were under greater residual compres-

sion, the oxygen-treated fibers possessed higher average strengths. In Fig. 5 the area between the dashed lines indicates the expected range of strengths available to date for B/W fibers whose fractures are core-initiated.

Turning now to the B/C fiber types, the tensile results of Table IV show that in the as-produced condition these fibers displayed better tensile properties than the majority of B/W fibers. After slight polishing, however, the B/C fibers showed only small improvement so that their properties became only comparable to those of the significantly improved LDSR B/W fibers. Fracture surface observations indicated that the source of this small polishing effect was the fact that the predominate fatal flaw for the B/C fibers was located not on the fiber surface but near the interface between the sheath and the pyrolytic graphite coating on the carbon core. Thus the strength properties after polishing were primarily controlled by this interface flaw. To determine whether it like the core flaw could be compressed and strengthened by contraction treatments, the 4C and 5.6C fiber types were subjected to deep polishing. The strength results listed in Table VII fail to show any trend which would indicate either an increase or decrease in the stress level or variability for interface-initiated fracture. Thus, if the B/C fibers are to be strengthened above current levels, the approach to be taken is not by secondary treatments involving contraction, but rather by primary treatments by which the manufacturer reduces the size and incidence of the interface flaw.

Summarizing the overall practical implications of the strengthening results, if optimum tensile strength properties are desired without chemical polishing, the as-produced B/C fibers are to be preferred over the majority of as-produced B/W fibers. The higher strength of these fibers is related to their relative surface smoothness and to the high stresses required for interface-initiated fracture. However, if the fibers are to be utilized for strength-critical and/or impact-critical composite applications, slighty-polished LDSR B/W fibers appear to offer considerable advantages over either the as-produced or polished B/C fiber types. These advantages lie not only in higher strength and lower variability, but also in the availability of larger diameters and in the capability of controlling and obtaining further strength improvement by the application of fiber contraction treatments.

Strength After Aluminum Reaction

To understand the extent to which the excellent strength characteristics of the LDSR boron fibers could be retained in B/Al composites, as-produced and polished type 8W fibers were ion plated with aluminum, thermally treated for 1 hour at B/Al fabrication temperatures, and then tensile tested at room temperature. The tensile strength results are listed in Table VIII. Because of its low modulus and small thickness, the aluminum coating was assumed to carry no load and the specimen diameter was taken as that of the base fiber before coating. For comparison purposes Table VIII also includes the strength properties measured before and after ion plating and prior to thermal treatment. In all cases these data support the fact that plating temperatures were not high enough to cause any strength loss in the base fiber.

The results of Table VIII indicate that generally above 450° C (840° F) the aluminum-coated fibers began to show evidence of strength degradation.

The source of this degradation was likely related to a thermally-induced boron-aluminum reaction occurring on the fiber surface. The $\bar{\sigma}_1$ results for the as-produced and pre-polished fibers are plotted in Fig. 6 as a function of the temperature for 1-hour thermal treatment. The solid curve is a best fit through the as-produced data. The dashed curve for pre-polished data was drawn on the assumption that this data set differed from the as-produced data set by a constant multiplicative factor (to be discussed). For these curves it was also assumed that at temperatures below the measurement range, $\bar{\sigma}_1$ remained unchanged from the 20° C (70° F) value which was measured after aluminum coating but before thermal treatment.

The Fig. 6 solid curve for as-produced fibers indicates that the 8W fibers with initial strengths near 4.2 GN/m^2 (610 ksi) had a threshold temperature for strength degradation near 470° C (880° F). Presumably at this temperature the average stress required to initiate fiber fracture from reaction-induced surface flaws decreased to a level equal to that required for fracture from strength-limiting flaws in the as-produced fibers. As temperature increased above 470° C (880° F) a monotonic decrease in $\bar{\sigma}_1$ occurred, indicating increased control of fiber fracture by reaction flaws and a general reduction in the stresses required for these flaws to initiate fraction. In support of the generality of this degradation curve for as-produced fibers, data obtained from the B/Al composite results of Klein and Metcalfe (8) are also plotted in Fig. 6. These $\bar{\sigma}_1$ data were calculated from average fracture strain results for 1 hour thermally-treated B/Al composite reinforced by 100 and 142 μm (4 and 5.6 mil) B/W fibers. A fiber modulus of 400 GN/m^2 (58 Msi) was assumed for these calculations which are based on Klein and Metcalfe's observation that for a gauge length of 25 mm (1 in.), the average fracture strain of fibers extracted from the composites agreed quite well (within ±10 percent) with the average composite fracture strain in the axial direction.

Because of the higher initial strength of the pre-polished 8W fibers, their threshold temperature for strength degradation was expected to be lower than that of the as-produced 8W fibers. However, as shown in Fig. 6, this was not the case. In fact pre-polishing somehow significantly increased the average stress levels required for reaction-induced surface flaws to initiate fiber fracture, and thereby shifted the pre-polished degradation curve to higher temperatures. The threshold temperature for slightly polished 195 μm (7.7 mil) fibers was near 515° C (960° F) some 45° C (80° F) higher than that of as-produced fibers plated and heated in an identical manner, and some 55° C (100° F) higher than one might expect from extrapolation of the as-produced degradation curve. The only obvious physical differences between the fibers were the initial surface structure and a possible small axial contraction of the pre-polished fibers during thermal treatment near 500° C (930° F) (6). However this latter effect can be neglected because the estimated strength increases are very small, 0.01 to 0.06 GN/m^2 (~2 to 9 ksi) and also because contraction should only affect intrinic fiber flaws which did not control fiber fracture during aluminum reaction. Thus the higher strengths of the reacted pre-polished fibers must be related to their initial surface structure.

To better understand this surface effect, bend test measurements were made on as-produced and pre-polished fibers treated in the same manner as those of Table VIII. The flexure strength results are listed in Table IX, again calculated by neglecting aluminum coating effects. Also included in

Table IX is L*, the effective fiber gauge length for each bend test group calculated under the assumption of only surface-initiated fractures (cf. Appendix A). As with the tensile results the flexure data showed that the ion-plating process itself caused no strength degradation of the base fiber and that thermal treatment above 450° C (840° F) caused a measurable drop in $\bar{\sigma}_b$. In order to plot this behavior, it was felt tha the $\bar{\sigma}_b$ data could not be used directly since they were measured at varying L*. To account for this effect, values for the average strength $\bar{\sigma}_1$ to be expected at L* = 2.5 mm (0.1 in.) were calculated by extrapolating the σ_b data according to Eqs. (2) and (A7). Because the L* of the bend tests were very nearly equal to 2.5 mm (0.1 in.) errors in the extrapolation method were considered to be minimal. The $\bar{\sigma}_1$ results for both as-produced and pre-polished fibers are listed in the last column of Table IX and are also plotted in Fig. 7 which displays the flexure data in a manner similar to that used for Fig. 6.

From Fig. 7 one notes that similar to the tensile results, under all thermal conditions examined the flexure strengths of the pre-polished fibers were measurably greater than those of the as-produced fibers. However, unlike the tensile results, fiber fracture in bending was presumably initiated only by surface flaws, so that the Fig. 7 data are a more direct manifestation of the strength advantages of the chemically-polished surface both before and after reaction. The predominance of surface-initiated fractures also allows one to examine directly the effects of aluminum reaction. The Fig. 7 flexure data indicate that both fiber types showed initiation of reaction-induced strength degradation at temperatures below their threshold for tensile degradation. This was particularly obvious for the pre-polished fibers whose $\bar{\sigma}_1$ dropped significantly from about 12 GN/m^2 (1700 ksi) at room temperature to approximately 7 GN/m^2 (1000 ksi) at 515° C (960° F). Thus the degradation effects of the aluminum reaction were indeed greater for the pre-polished fibers, but because of their high initial strengths, the dropoff near 500° C (930° F) was still not large enough to yield $\bar{\sigma}_1$ as low as those of the reacted as-produced fibers. On the basic side, this result suggests that the higher strengths of the reacted pre-polished fibers were probably not caused by a reduction in aluminum reaction rate but rather by a reduction in the detrimental effects of the as-produced surface structure on flaws associated with the boron-aluminum reaction product. On the practical side, it suggests that in a B/Al composite the pre-polished fibers should have adequate fiber-matrix bonding for mechanical load transfer at or below their threshold temperature for tensile degradation.

Both the tensile and flexure results for the reacted fibers support the fact that conditions on the as-produced surface somehow decreased the stress levels required for reaction-induced surface flaws to initiate fiber fracture. The exact surface structure responsible for this effect was not identified. However, the fact that only slight polishing was needed to significantly reduce its detrimental effects suggests that curvature at the nodule boundaries may play an important role (cf. discussion of Fig. 3). Nevertheless, whatever the responsible source, one can empirically describe its effects by assuming it raises the applied stress on reaction flaws by a constant factor K. By calculating the ratio of pre-polished to as-produced strength at temperatures for reaction-controlled fracture, one obtains an average K value of 1.6 for both the tensile and flexure data. Assuming

the as-produced fibers degraded by the solid curves of Figs. 6 and 7, the fit of this K value through the pre-polished data is shown by the dashed curves. Thus the data near 500° C (930° F) support an empirical model in which the as-produced surface increased the applied stress on reaction flaws by some 60 percent.

Composite Implications

Chemical polishing of the type 8W boron fibers not only improved fiber strength and reduced variability but also allowed retention of these desirable characteristics to higher temperatures when in contact with aluminum. This latter finding could have very significant implications for the fabrication of high performance B/Al composites. It suggests, for example, that higher fabrication temperatures could be employed without affecting fiber tensile strength properties. B/Al composites are typically consolidated by diffusion bonding at temperatures between 455° and 510° C (850° and 950° F) in order to minimize reaction-related fiber degradation and still obtain adequate aluminum-aluminum bonding. Opening the temperature window for fabrication by a polishing pre-treatment should allow for greater flexibility in temperature control and also aid in consolidation of those aluminum alloys which require higher diffusion bonding temperatures.

Another important aspect of the chemical polish treatment is that in combination with the oxygen treatment it should result in B/Al composites with significantly higher strength than those currently being fabricated using as-produced fibers. To estimate this composite strengthening capability, Rosen's cumulative weakening theory (15) was used to calculate the average composite strengths to be expected by reinforcing 6061 aluminum alloy with as-produced, slightly-polished, and oxygen-strengthened type 8W fibers (cf. Appendix B). The results are listed in Table X for unidirectional composites fabricated at 480° and 510° C (900° and 950° F) with 50 percent fiber volume fraction. Also included in Table X are the assumed strength properties for the in-situ fibers and the calculated in-situ fiber bundle lengths δ (cf. Appendix B). The last column which compares composite strengths with that of the first composite fabricated at 480° C (900° F) clearly shows the potential strength and fabrication advantages to be gained by reinforcing with slightly-polished and oxygen-treated fibers.

It should be mentioned that although polished fibers should reduce degradation effects during B/Al fabrication, they cannot compare in this regard with commercially available boron fibers that are coated with diffusion barriers such as silicon carbide and boron carbide. These coated fibers, however, typically display lower strengths than uncoated as-produced fibers and are currently produced only in small diameters. Their low strength suggests a weak flaw structure in the barrier coating, or perhaps, a stress raiser effect of the coating by growth nodules on the base fiber. Thus, although the barrier-coated fiber types may simplify B/Al fabrication, they do not at the present time offer the significant strength and impact absorption advantages of the oxygen-treated and polished LDSR fibers.

CONCLUDING REMARKS

The results of this study show that for certain types of commercial boron fibers, the application of a simple chemical processing treatment can

not only cause a significant improvement in strength properties but can also assist in retaining these properties under thermal conditions typically encountered during the fabrication of B/Al composites.

A survey of various diameter fibers produced in different manners on both tungsten and carbon substrates indicated that the fiber types most improved by polishing were those with diameters from 203 to 406 μm (8 to 16 mil) that were deposited onto tungsten in a single CVD reactor. The strengths of these fiber types were limited only by flaws on the fiber surface and by flaws within the tungsten-boride core. After slight polishing, only the high-strength low-variability core flaws remained to control fiber fracture. In general this resulted in an increase in average tensile strength from about 3.4 GN/m^2 (500 ksi) to 4.4 GN/m^2 (640 ksi), a decrease in coefficient of variation from about 15 to 3 percent, and an increase in Weibull modulus from about 8 to 40. By applying contraction treatments such as the oxygen treatment, the stress required for core-initiated fracture could be raised to even higher levels. To date, average strengths have been increased to 5.5 GN/m^2 (800 ksi) while CV and Weibull modulus remained at 3 percent and 40, respectively.

From studies of the potential for retention of the fiber strength properties in B/Al composites, it appears that the surface structure of CVD commercial fibers not only has detrimental effects on as-produced fiber strength but also accentuates strength degradation effects associated with the thermally-induced boron-aluminum reaction that occurs during composite fabrication. This conclusion is based on the observation that after being aluminum coated and heat treated near 500° C (930° F), coated as-produced fibers display measurably lower tensile and flexure strengths than coated pre-polished fibers. These data suggest that the chemical polish treatment should allow B/Al composites to be fabricated successfully at temperatures as high as 510° C (950° F) for slightly-polished fibers and as high as 490° C (910° F) for oxygen-treated fibers. This should be accomplished with little loss of fiber strength properties or fiber/matrix bonding required for mechanical load transfer. Thus the chemical polish treatment in combination with the oxygen treatment and the larger diameter fibers offer potential for fabricating B/Al composites with strength and impact properties significantly greater than those currently available.

APPENDIX A

STATISTICAL ANALYSIS OF SURFACE-INITIATED FRACTURES

For those situations in which fiber fracture was controlled only by surface flaws, it was possible using Weibull theory to convert flexure strength results into tensile strength data at an effective gauge length L^*.

For example, assuming the stresses for surface-initiated fracture can be fitted to two-parameter Weibull theory (α and ω), the probability of survival P at an applied stress σ can be determined from

$$-\ln P = \alpha \int_S (\sigma)^\omega \, dS \tag{A1}$$

Here ω is Weibull modulus, α is a scale parameter, and S is the fiber surface area involved in the test. For tensile tests at constant gauge length L, σ is constant for all surface elements dS so that

$$-\ln P = \alpha\pi DL(\sigma)^\omega \tag{A2}$$

For the bend tests of this study, the applied surface stress varied according to $\sigma = \sigma_b \sin\theta$ where $\sigma_b = ED/2a$ is the maximum tensile stress for a test at cone radius a, θ is the cylindrical angle coordinate around the fiber axis, and E and D are the fiber modulus and diameter, respectively. The bend test length L_b also varied, obeying the relations

$$L_b = \pi a = \frac{\pi ED}{2\sigma_b} = \frac{\bar{L}_b \bar{\sigma}_b}{\sigma_b}. \tag{A3}$$

Here $\bar{\sigma}_b$ and $\bar{L}_b$ are the average values measured for bend fracture of the test group. Taking $dS = L_b D \, d\theta/2$, it follows from Eqs. (A1) and (A3) that the survival probability in the bend tests can be determined from

$$-\ln P = \alpha\pi D\bar{L}_b\bar{\sigma}_b\beta_\omega(\sigma_b)^{\omega-1} \tag{A4}$$

where $\beta_\omega = \int_0^\pi \sin^\omega\theta \, d\theta/2\pi$. The dependence of β_ω on the Weibull modulus is shown in Fig. 8.

Since the average strength is given by $\int_0^\infty \sigma \, dP$, it follows from Eqs. (A1), (A2), and (A4) that for the tensile tests

$$\bar{\sigma} = (\alpha\pi DL)^{-1/\omega} \, \Gamma[1 + 1/\omega] \tag{A5}$$

and for bend tests

$$\bar{\sigma}_b = (\alpha\pi D\beta_w \Gamma_b)^{-1/\omega}\, \Gamma[\omega/(\omega - 1)]^{(\omega-1)/\omega} \tag{A6}$$

Here Γ is the gamma function. For $\omega \geq 5$, the Γ functions of Eqs. (A5) and (A6) differ by less than 1 percent so that by comparing these equations it can be seen that $\bar{\sigma}_b$ was essentially equivalent to the average tensile strength that would be measured at $L^* = \bar{\beta}_\omega L_b = \beta_\omega \pi ED/2\bar{\sigma}_b$.

It also can be shown using Eq. (A2) that although the coefficient of variation (CV) for the tensile tests has a complicated dependence on Weibull modulus, this dependence can be approximated quite well by the relation $CV = 1.2/\omega$. Performing the same calculation for the bend test coefficient of variation $(CV)_b$, one finds using Eq. (A4) the same result as the tensile CV except with ω now replaced by $\omega - 1$. It follows then by the same tensile approximation, that

$$(CV)_b = \frac{1.2}{(\omega - 1)}. \tag{A7}$$

Thus due to the variation in L_b, the CV in bending was slightly larger than the CV in tension.

APPENDIX B

COMPOSITE STRENGTH THEORY

To obtain a good approximation for the axial tensile strength σ_c of a unidirectional metal matrix composite, one can employ Rosen's cumulative weakening theory (15) which predicts

$$\sigma_c = v_f \sigma_{Bf} + v_m \sigma_{ym}. \tag{B1}$$

Here v_f and v_m are the volume fracton of fiber and matrix, respectively; σ_{Bf} is the strength of a fiber bundle of length δ; and σ_{ym} is the tensile yield strength of the matrix. For a ductile matrix like aluminum, the bundle length can be calculated from

$$\delta = \frac{\sigma D}{2\tau_{ym}} \tag{B2}$$

where $\sigma = \sigma_{Bf}$, D is fiber diameter, and τ_{ym} the shear yield strength of the matrix. Assuming a large number of fibers governed by two-parameter Weibull statistics, the bundle strength at length δ can be determined from the average fiber strength $\bar{\sigma}_L$ measured for individual fibers of length L:

$$\sigma_{Bf} = \bar{\sigma}_L (L/\delta)^{1/\omega} [(\omega e)^{-1/\omega}/\Gamma(1 + 1/\omega)] \tag{B3}$$

where Γ is the gamma function, e is the natural base constant, and ω is the Weibull modulus (12).

REFERENCES

1. L. E. Dardi and K. G. Kreider; pp. 231-270 in Failure Modes in Composites. Edited by I. Toth. The Metallurgical Society of AIME, New York, 1973.
2. C. C. Chamis and M. P. Hanson, and T. T. Serafini; pp. 324-349 in Composite Materials: Testing and Design (Second Conference), (ASTM STP 497). American Society for Testing and Materials, Philadelphia, 1972.
3. V. Krukonis; pp. 517-540 in Boron and Refractory Borides. Edited by V. I. Matkovich. Springer-Verlag, Berlin, 1977.
4. R. J. Smith, "Changes in Boron Fiber Strength due to Surface Removal by Chemical Etching," NASA TN D-8219, 1976.
5. D. R. Behrendt; pp. 215-226 in Composite Materials: Testing and Design (Fourth Conference), (ASTM STP 617). American Society for Testing and Materials, Philadelphia, 1977.
6. J. A. DiCarlo, "Techniques for Increasing Boron Fiber Fracture Strain," NASA TM X-73627, 1977.
7. J. A. DiCarlo and T. C. Wagner, "Oxidation-Induced Contraction and Strengthening of Boron Fibers," NASA TM-82599, 1981.
8. M. J. Klein and A. G. Metcalfe, "Effect of Interfaces in Metal Matrix Composites on Mechanical Properties," AFML-TR-71-189, 1971.
9. Street, K. N. and J. P. Ferte; pp. 137-163 in ICCM, First International Conference on Composite Materials. The Metallurgical Society of AIME, New York, 1976.
10. D. L. McDanels and R. A. Signorelli; pp. 27-57 in Failure Modes in Composites III. The Metallurgical Society of AIME, New York, 1976.
11. T. Spalvins, "Horizons in Ion Plated Coatings," Metal Finishing, 72 [6] 38-43 (1974).
12. H. T. Corten; pp. 27-105 in Modern Composite Materials. Edited by L. Broutman and R. Krock. Addison-Wesley, Reading, Mass., 1967.
13. F. E. Wawner, Jr.; pp. 283-300 in Boron, Volume 2 - Preparation Properties, and Applications. Edited by G. K. Gaule. Plenum Press, N.Y., 1965.
14. J. Vega-Boggio, O. Vingsbo, and J. Carlsson, "The Initial Stages of Growth and the Origin of Proximate Voids in Boron Fibers," J. Mater. Sci., 12 [9] 1750-1758 (1977).
15. B. W. Rosen, "Tensile Failure of Fibrous Composites," AIAA Journal, 2 [11] 1985-1991 (1964).

TABLE I. - TYPES OF BORON FIBER SPECIMENS

As-produced diameter, μm (mils)	Substrate[a]	Production method[b]	Commercial source	Identification
102 (4)	W	SRSS	AVCO	4W
142 (5.6)	W	SRSS	AVCO	5.6W
203 (8)	W	SRSS[c]	AVCO	8W
	W	DRSS	AVCO	$\overline{8W}$[d]
203 (8)	W	SRMS	CTI[e]	8W*[e]
279 (11)	W	SRMS	CTI	11W*
406 (16)	W	SRMS	CTI	16W*
102 (4)	C	SRSS	AVCO	4C
142 (5.6)	C	SRSS	AVCO	5.6C

[a]W = tungsten, C = carbon.
[b]SRSS = single reactor with single stage
DRSS = double reactor with single stages
SRMS = single reactor with multiple stages.
[c]SRSS augmented by high frequency heating.
[d]Double reactor fiber
[e]Asterisk indicates fibers produced by Composites Technology Inc. CTI.

TABLE II. - TENSILE STRENGTH RESULTS FOR AS-PRODUCED AND POLISHED TYPE 8W BORON FIBERS

Gauge length, mm[a]	Diameter ratio, D/D_o	Average strength, $(GN/m^2)^a$	Coefficient of variation, percent	Maximum strength	Minimum strength	Number of specimens
				$(GN/m^2)^a$		
25	1.00[b]	3.45	21	4.56	2.01	29
	.98	4.40	3	4.55	4.23	10
	.93	4.57	3	4.81	4.27	21
	.81	4.92	2	5.03	4.72	14
	.69	5.03	3	5.27	4.76	10
	.56	5.23	5	5.53	4.70	11
250	.93	4.44	3	4.86	4.17	21

[a]1 mm = 0.04 in., 1 GN/m^2 = 145 ksi.
[b]As-produced condition (D_o = 203 μm = 8 mil).

TABLE III. - FLEXURE STRENGTH RESULTS FOR AS-PRODUCED

AND POLISHED TYPE 8W BORON FIBERS

Diameter ratio, D/D_o	Average strength, $(GN/m^2)^a$	Coefficient of variation, percent	Maximum strength	Minimum strength	Number of specimens
			$(GN/m^2)^a$		
1.00[b]	5.95	7	6.67	5.08	20
.99	9.36	3	13.10	6.16	7
.96	12.53	15	15.65	7.89	10
.80	12.23	34	16.69	3.81	12
.74	11.88	32	15.63	4.62	10

[a]1 GN/m^2 = 145 ksi.
[b]As-produced condition (D_o = 203 μm = 8 mil).

TABLE IV. - TENSILE STRENGTH RESULTS FOR VARIOUS TYPES OF BORON FIBERS

		As-produced			Slightly-polished				
Type	Gauge length, mm[a]	Average strength, $(GN/m^2)^a$	Coefficient of variation, percent	Number of specimens	Diameter ratio, D/D_o	Average strength, $(GN/m^2)^a$	Coefficient of variation, percent	Number of specimens	Fatal flaw sites[b]
4W	25	3.32	10	20	0.84	3.66	14	9	ci,c
5.6W	25	2.88	14	19	.88	3.28	13	10	ci,c
8W	25	3.45	21	29	.93	4.57	3	21	c
	250				.93	4.44	3	21	c
8W	250	2.74	20	10	.94	3.76	12	10	ri,c
8W*	25	4.03	7	14	.93	4.38	3	60	c
11W*	25	3.63	12	10	.93	4.22	4	9	c
16W*	25	(2.06)[c]	14	18	.94	4.65	4	11	c
4C	25	4.20	8	41	.86	4.47	4	11	ci
5.6C	25	4.02	16	30	.91	4.42	9	10	ci

[a]1 mm = 0.04 in., 1 GN/m^2 = 145 ksi.
[b]Fatal flaw sites: c - core
ci - core-sheath interface
ri - double-reactor interface.
[c]All fractures occurred at edge of grips.

TABLE V. - TENSILE STRENGTH RESULTS FOR AS-PRODUCED

AND POLISHED LARGE DIAMETER BORON FIBERS

Type	Diameter ratio, D/D_o	Average strength,[a] (GN/m^2)[b]	Coefficient of variation, percent	Maximum strength	Minimum strength	Number of specimens
				(GN/m^2)[b]		
8W*	1.00[c]	4.03	7	4.35	3.50	14
	.93	4.38	3	4.65	4.00	60
	.83	4.57	4	4.85	4.22	15
	.77	4.55	5	4.95	4.05	15
	.58	4.81	5	5.11	4.41	10
11W*	1.00[c]	3.63	12	4.27	3.19	10
	.93	4.22	5	4.52	3.89	9
	.79	4.58	2	4.68	4.42	7
	.71	4.69	4	4.90	4.39	7
	.52	4.72	6	5.18	4.34	10
16W*	1.00[c]	(2.06)[d]	14	(2.47)[d]	(1.48)[d]	18
	.94	4.65	4	4.83	4.23	11
	.89	4.97	2	5.07	4.84	5
	.74	5.17	6	5.34	4.65	5
	.53	5.66	6	6.06	5.19	8

[a]Average tensile strength at gauge length of 25 mm (1 in.)
[b]1 GN/m^2 = 145 ksi.
[c]As-produced condition.
[d]All fractures occurred at edge of grips.

TABLE VI. - TENSILE STRENGTH RESULTS FOR OXYGEN-TREATED

AND POLISHED LARGE DIAMETER BORON FIBERS

Type	Axial contraction, ϵ_z, percent	Diameter ratio, D/Do	Average strength,[b] (GN/m^2)[c]	Coefficient of variation, percent	Number of specimens
8W	0.28	0.88	5.54	3	5
11W*	.29	.93	5.40	5	4
16W*	.24	.94	5.68	4	4

[a]Axial contraction strain during oxidation treatment.
[b]Average tensile strength at gauge length of 25 mm (1 in.).
[c]1 GN/m^2 = 145 ksi.

TABLE VII. - TENSILE STRENGTH RESULTS FOR AS-PRODUCED AND POLISHED BORON ON CARBON FIBERS

Type	Diameter ratio, D/D_o	Average strength,[a] $(GN/m^2)^b$	Coefficient of variation, percent	Maximum strength	Minimum strength	Number of specimens
				$(GN/m^2)^b$		
4C	1.00[c]	4.20	8	4.63	3.19	41
	.93	4.47	4	4.83	4.18	11
	.83	4.40	7	4.98	4.03	12
	.77	4.21	5	4.60	3.92	16
5.6C	1.00[c]	4.02	16	4.76	3.11	30
	.90	4.42	9	5.22	3.56	10
	.77	3.82	29	4.67	1.90	10
	.67	4.29	9	5.27	3.34	12

[a]Average tensile strength at gauge length of 25 mm (1 in.).
[b]1 GN/m^2 = 145 ksi.
[c]As-produced condition.

TABLE VIII. - TENSILE STRENGTH RESULTS FOR HEAT-TREATED ALUMINUM COATED TYPE 8W BORON FIBERS

Treatment temperature		Average strength,[a] $(GN/m^2)^b$	Coefficient of variation, percent	Maximum strength	Minimum strength	Number of specimens
°C	°F			$(GN/m^2)^b$		
D_o = 203 μm (8.0 mil as-produced)						
As-produced		3.45	21	4.56	2.01	29
Al coated		4.24	8	4.49	3.23	13
450	842	4.24	5	4.51	3.86	5
466	871	4.17	12	4.59	3.49	5
476	889	4.01	14	4.49	2.71	10
485	905	3.64	7	4.06	3.35	5
490	914	3.29	18	4.02	2.22	9
512	954	2.90	14	3.52	2.24	10
527	981	2.65	21	3.42	1.53	10
D = 195 μm (7.7 mil)						
Polished		4.40	2	4.55	4.23	10
Al coated		4.57	1	4.58	4.54	3
515	959	4.42	6	4.66	3.91	5
527	981	4.09	10	4.60	3.57	5
538	1000	3.91	13	4.34	2.99	5
D = 180 μm (7.1 mil)						
Polished		4.57	3	4.81	4.26	21
Al coated		4.56	3	4.87	4.25	13
504	939	4.89	4	5.20	4.50	12
520	968	3.94	18	4.93	2.39	12
527	981	4.17	14	4.77	2.79	10
D = 140 μm (5.5 mil)						
Polished		5.03	3	5.27	4.76	10
Al coated		5.02	2	5.12	4.88	5
509	948	4.82	14	5.70	3.49	9
550	1022	3.20	20	4.32	1.91	11

[a]Average tensile strength at gauge length of 25 mm (1 in.).
[b]1 GN/m^2 = 145 ksi.

TABLE IX. - FLEXURE STRENGTH RESULTS FOR HEAT-TREATED ALUMINUM-COATED TYPE 8W BORON FIBERS

Treatment temperature		Average strength, $(GN/m^2)^a$	Coefficient of variation, percent	Maximum strength	Minimum strength	Number of specimens	Effective gauge length, L^*, mm[a]	Predicted strength $L^* = 2.5$ mm, $(GN/m^2)^a$
°C	°F			$(GN/m^2)^a$				
D_o = 203 um (8.0 mil as-produced)								
As-produced		-----	--					
Al coated		6.77	11	8.18	5.32	22	2.2	6.70
450	842	6.00	7	6.65	4.83	10	2.1	5.94
466	871	6.16	6	6.65	5.60	9	1.7	6.06
476	889	5.97	8	6.65	5.06	15	2.2	5.92
485	905	5.52	15	6.26	3.80	9	3.2	5.67
490	914	5.00	15	6.26	3.94	19	3.5	5.19
512	954	4.63	14	5.91	3.94	15	3.6	4.80
527	981	4.04	12	4.83	3.22	11	3.9	4.21
D = 195 um (7.7 mil)								
Polished		12.53	14	14.65	7.89	10	1.2	11.64
Al coated		13.78	10	14.59	11.35	4	.9	12.81
515	959	6.79	23	10.10	4.62	7	2.8	6.92
527	981	5.74	10	6.37	5.02	7	2.3	5.70
538	1000	6.10	15	7.79	5.09	6	2.6	6.13
D = 180 um (7.1 mil)								
Polished		-----	--					
Al coated		12.67	16	16.07	8.56	17	1.2	11.62
504	939	8.39	12	9.44	5.86	9	1.6	8.06
520	968	5.78	23	8.49	3.79	14	3.1	5.99
527	981	6.36	25	9.63	3.78	18	2.8	6.48
D = 140 um (5.5 mil)								
Polished		10.03	40	15.22	6.33	5	1.7	9.11
Al coated		11.32	44	18.40	2.80	9	1.5	9.96
509	948	8.27	39	16.35	4.28	14	2.0	7.82
527	981	5.64	27	8.64	2.97	11	2.6	5.68
550	1022	5.43	31	9.10	2.61	13	2.8	5.55

[a] 1 mm = 0.04 in., 1 GN = 145 ksi.

TABLE X. - PREDICTED TENSILE STRENGTHS OF UNIDIRECTIONAL B/Al COMPOSITES[a]

Fiber treatment	One-hour fabrication temperature, °C (°F)	In-situ fiber properties					Composite strength		
		Average strength at 25 mm (1 in.)		Coefficient of variation, percent	Weibull modulus, ω	Bundle length, δ, mm	σ_c		Percent difference
		GN/m²	ksi				GN/m²	ksi	
As-produced	480 (900)	3.7	540	15	8	3.5	1.75	253	±0
	510 (950)	3.0	440	15	8	2.9	1.45	211	-17
Slight polish	510 (950)	4.6	670	3	40	4.4	2.20	319	+26
Oxygen + polish	480 (900)	5.5	800	3	40	5.2	2.61	379	+50

[a]Assumed constituent properties:
Fiber: 203 μm (8 mil), type 8W at 50 percent volume fraction.
Matrix: 6061 aluminum: shear yield strength = 0.1 GN/m²
tensile yield strength = 0.06 GN/m².

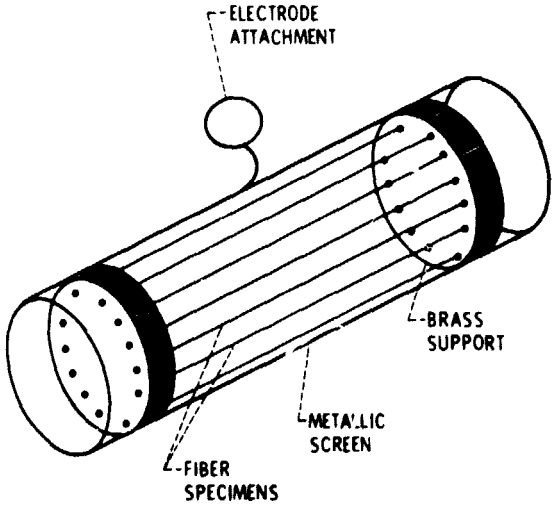

Figure 1. - Schematic of specimen holder for ion-plating.

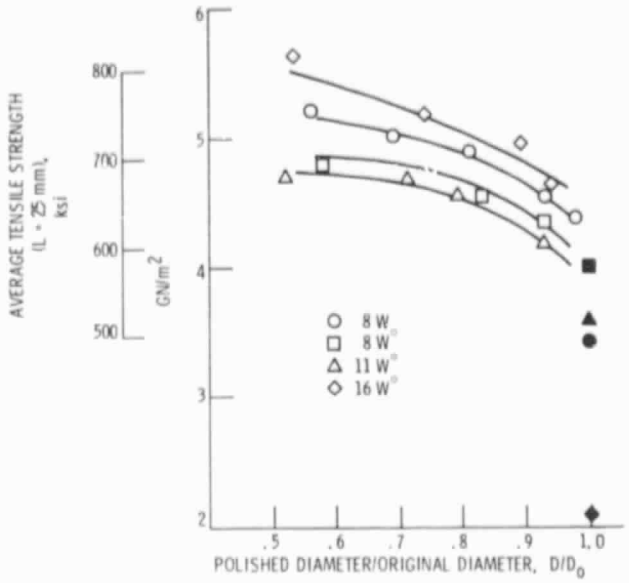

Figure 2. - Effects of deep chemical polishing on the tensile strength of large diameter boron on tungsten fibers.

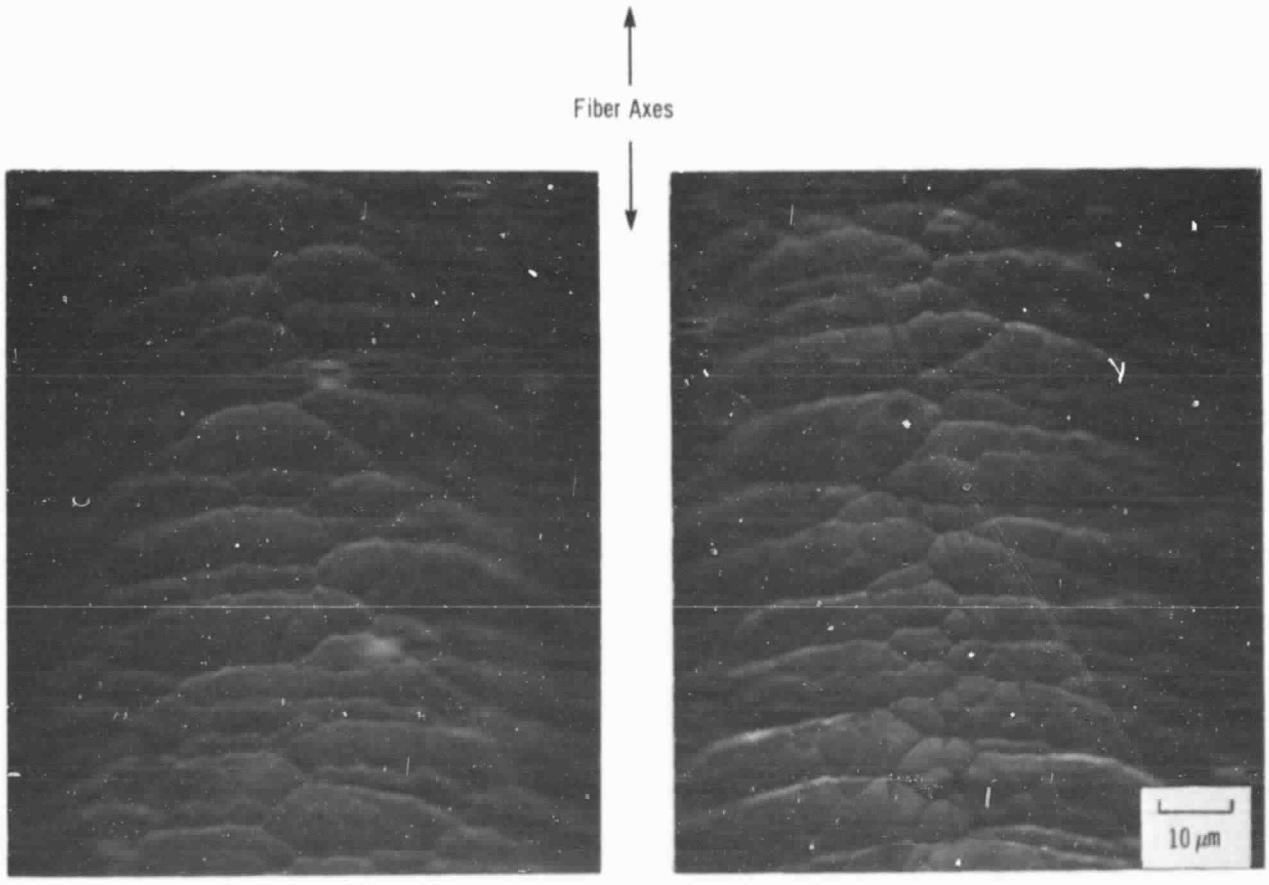

(a) As-produced (Diam = 203 μm, flex strength = 6 GN/m^2)

(b) Polished (Diam = 193 μm, flex strength = 12 GN/m^2)

Figure 3. - Optical micrographs of the surface type 8W boron fibers before and after slight chemical polishing.

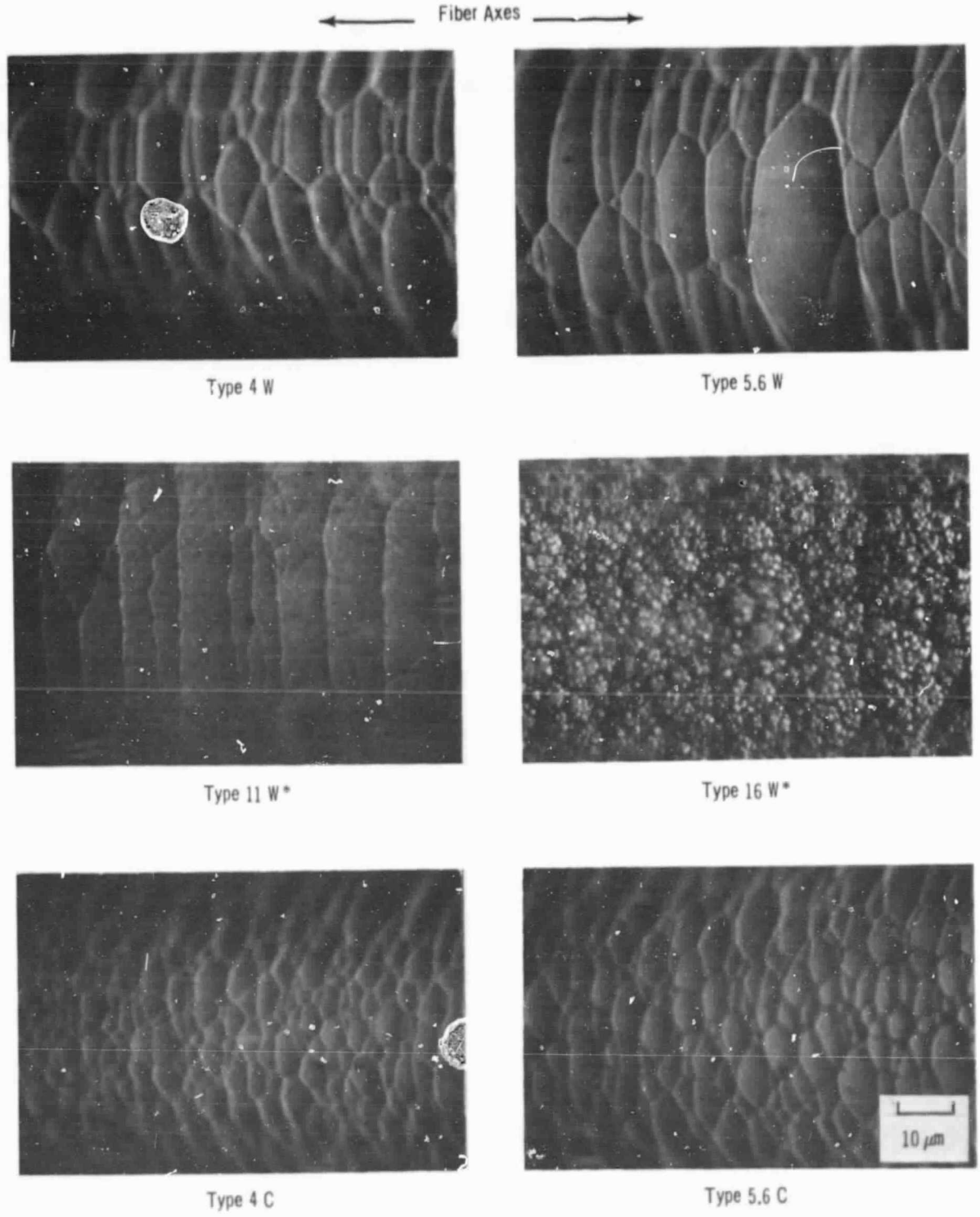

Figure 4. - Optical micrographs of the as-produced surfaces of different types of boron fibers.

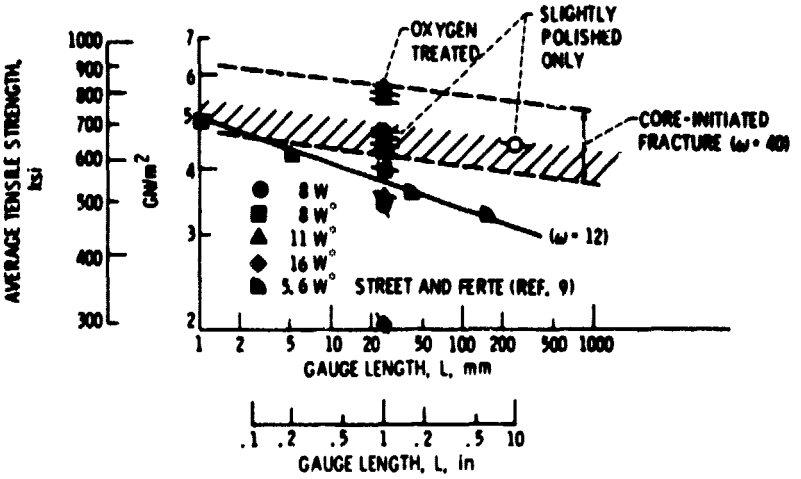

Figure 5. - Predicted gauge length effects for the average strengths of as-produced (closed points) and slightly polished (open points) boron on tungsten fibers.

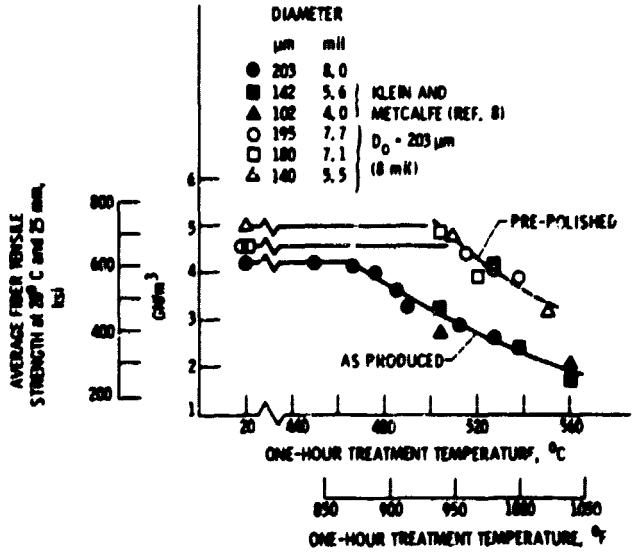

Figure 6. - Effects of one-hour treatments on the room temperature tensile strength of aluminum-coated type SW boron fibers.

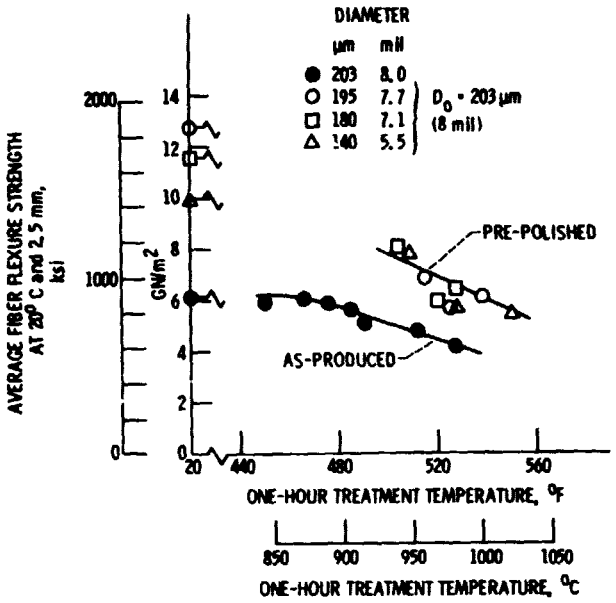

Figure 7. - Effects of one-hour heat treatments on the room temperature flexure strength of aluminum-coated type SW boron fibers.

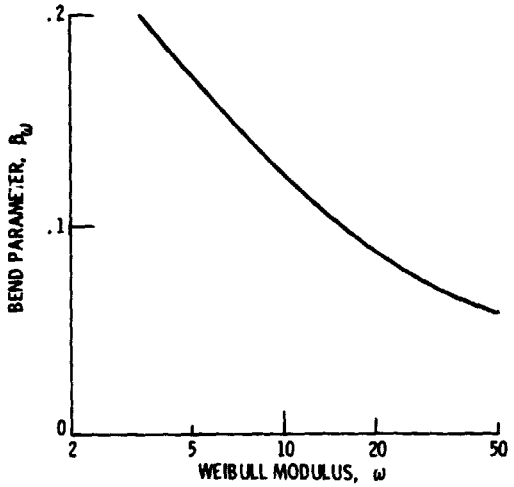

Figure 8. - Dependence of β parameter on Weibull modulus.